Integrated 3D porous C-MoS$_2$/nitrogen-doped graphene electrode for high capacity and prolonged stability lithium storage

D. Xie, W.J. Tang, X.H. Xia, D.H. Wang, D. Zhou, F. Shi, X.L. Wang, C.D. Gu, J.P. Tu[*]

State Key Laboratory of Silicon Materials, Key Laboratory of Advanced Materials and Applications for Batteries of Zhejiang Province, and School of Materials Science & Engineering, Zhejiang University, Hangzhou 310027, China

HIGHLIGHTS

- The C-MoS$_2$/N-G integrated electrode is synthesized by a hydrothermal-induced method.
- The preformed C-MoS$_2$ is strongly anchored on the porous N-doped graphene aerogel.
- The superior performance is attributed to the porous graphene scaffold and N-doping effect.
- The storage mechanism of the C-MoS$_2$/N-G integrated electrode is investigated in detail.

GRAPHICAL ABSTRACT
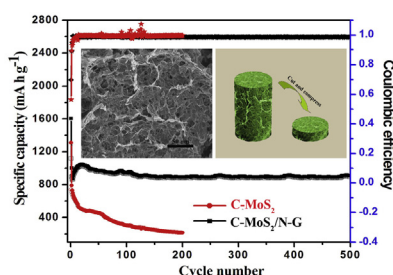
ABSTRACT

Scrupulous design and fabrication of advanced anode materials are of great importance for developing high-performance lithium ion batteries. Herein, we report a facile strategy for construction of free-standing and free-binder 3D porous carbon coated MoS$_2$/nitrogen-doped graphene (C-MoS$_2$/N-G) integrated electrode via a hydrothermal-induced self-assembly process. The preformed carbon coated MoS$_2$ is strongly anchored on the porous nitrogen-doped graphene aerogel architecture. As an anode for lithium ion batteries, the C-MoS$_2$/N-G electrode delivers a high first discharge capacity of 1600 mAh g^{-1} and maintains 900 mAh g^{-1} after 500 cycles at a current density of 200 mA g^{-1}. Impressively, superior high-rate capability is achieved for the C-MoS$_2$/N-G with a reversible capacity of 500 mAh g^{-1} at a high current density of 4000 mA g^{-1}. Furthermore, the lithium storage mechanism of the obtained integrated electrode is investigated by ex-situ X-ray photoelectron spectroscopy and transmission electron microscopy in detail.

© 2015 Elsevier B.V. All rights reserved.

1. Introduction

Rechargeable lithium ion batteries (LIBs) have been widely studied for energy storage applications, such as portable electronic devices, hybrid electric vehicles and electric vehicles [1–3]. Graphite, as the commercially available anode material, cannot fully meet the requirements for high-energy LIBs application due to its relatively small theoretical capacity (372 mAh g^{-1}) [4]. Thus, graphite should be replaced by alternative higher capacity materials for the next generation LIBs. Among the multitudinous explored materials, the graphene-like layered MoS$_2$ has attracted particular attention due to its high theoretical capacities (~670 mAh g^{-1}) and safer operation [5–7]. It consists of atomic layers of S-Mo-S stacked together by Van der Waals interactions. Such layered structure allows small ions to be reversibly

intercalated into the galleries between layers without large volume expansion in its overall dimension [7–9]. However, the further application of graphene-like MoS_2 LIBs is impeded by its inherent limitations [10–13]. First, this semiconductor MoS_2 has inherently low electronic conductivity affecting its electrochemical performance for lithium ion storage. Second, the adjacent graphene-like layer can be easily restacked together under the Van der Waals interactions during charge/discharge processes. Furthermore, the volume expansion and mechanical stress as a concomitant of lithium ion insertion and extraction can induce the failure of the electrode and the loss of contact between the active material and current collector, resulting in fast fading of reversible capacity.

To circumvent these challenges, canbonaceous materials have established themselves as promising candidates [14–16]. As one of the special structures of carbon consisting of monolayers of hybridized carbon atom arrange in a honeycombed network with six-membered rings, the two dimensional (2D) graphene is the most promising matrix for supporting the graphene-like MoS_2 because of high chemical stability, high electrical conductivity and good flexibility [17–21]. For example, the nanotile-like MoS_2-graphene hybrid synthesized by a Gemini surfactant assisted hydrothermal route exhibited much higher reversible capacity with significantly enhanced cyclic stability and rate capability than the pristine MoS_2 [22]. The graphene sheets could restrict the stacking of MoS_2 and promote fast electron transport between the MoS_2 layer and current collector. Although improved electrochemical properties have been observed, there are some disadvantages existing for lithium storage in these hybrids. The few-layer MoS_2 nanosheets are still prone to strong aggregation during charge/discharge process due to the non-intimate contact between the graphene layer and active materials. In addition, the large contact resistance exists among numerous active nanosheets. Fortunately, three dimensional (3D) graphene with porous interconnected framework and large specific surface area has been provided a path for settling this issue and developed for lithium storage. For example, Yang et al. developed 3D graphene network-backboned MoS_2-graphene composite by different approaches [3,23]. These optimal MoS_2-graphene architectures exhibited high reversible capacities (about 1200 mAh g^{-1}) and good rate performance.

Furthermore, chemical doping, especially nitrogen-doping of graphene was an effective way to enhance the lithium storage performance of graphene based composite because nitrogen doping can modulate the electronic structure of graphene, create defects to decrease the energy barrier of Li ion penetration and improve reactive sites [24–28]. Chang et al. synthesized ultrathin MoS_2/nitrogen-doped graphene and this hybrid exhibited superior cyclic stability and high-rate capability [29]. Considering that 3D porous interconnected framework and nitrogen doping of graphene can greatly improve the lithium storage properties, it is highly demanded to develop MoS_2-graphene hybrid as an anode for LIBs that combine the two characteristics together.

Herein, the 3D porous carbon coated MoS_2/N-doped graphene (C-MoS_2/N-G) integrated electrode is constructed via a hydrothermal-induced self-assembly process using the C-MoS_2 nanosheet sol as a precursor. As shown in Scheme 1, the C-MoS_2/N-G aerogel is easily synthesized by mixture of homogeneous C-MoS_2 nanosheets and graphite oxide solution, and subsequent hydrothermal reaction. The pH value is controlled by adding appropriate amount of ammonia ($NH_3 \cdot H_2O$) for conversion of graphite oxide to graphene. Graphene could curl and cross-like to form a 3D framework during dehydration due to the combination of hydrophobic nature and $\pi-\pi$ interaction while the MoS_2 nanosheet was embedded into the galleries of graphene [30]. Furthermore, $NH_3 \cdot H_2O$ can further enhance this assemble in a compact manner and acts as nitrogen sources for N-doping of 3D graphene, requiring

no additional nitrogen-containing precursor or and post treatment [24,31]. The procedure is detailed in the experimental section. The resulting C-MoS_2/N-G aerogel benefits from the synergistic effects of their each component: 1) graphene could effectively prevent C-MoS_2 nanosheets from complete restacking and aggregation, and vice versa, therefore facilitating the ultrafast diffusion of lithium ions/electrons within the electrode; 2) the excellent electrical and mechanical properties of 3D porous graphene can not only improve the conductivity of hybrid aerogel but also accommodate the volume change of electrode during charge/discharge process; 3) Nitrogen-doping of graphene can modulate the electronic structure of graphene-based composite and further improve the lithium storage properties. As a result, the as-prepared C-MoS_2/N-G aerogel exhibits superior cycling stability and rate capability compared with the C-MoS_2 nanosheets.

2. Experimental

2.1. Preparation of C-MoS_2 nanosheets

Typically, 0.164 g PEG-20000 was dissolved and stirred for 15 min in 60 mL deionized water to form clear solution, followed by the addition of 1.2 g $Na_2MoO_4 \cdot 2H_2O$ and 1.56 g of CH_3CSNH_2. The resulting solution was stirred for 30 min at room temperature by using a magnetic stirrer. And then it was transferred into a 100 mL Teflon-lined stainless steel autoclave and annealed at 200 °C for 24 h. After that, the precipitate was collected by centrifugation, wash with deionized water for three times, and then freeze-dried.

2.2. Preparation of graphene oxide (GO) dispersion

GO was prepared from natural graphite powder by a modified Hummers' method [17,32]. In general, 1.0 g of natural graphite powder was added to the solution of concentrate H_2SO_4/HNO_3 (92/23 mL) and then 3.0 g of $KMnO_4$ was added gradually under constant stirring. The resulting mixture was kept in an ice bath for 2 h. After removing the ice bath, it was stirred at 35 °C for 2 h. And then, 46 mL of deionized water was added into the mixture. Subsequently, the mixture was kept at 98 °C for 1 h and 10 mL of 30 wt % H_2O_2 was added into it when cooled to the room temperature naturally. The color of the mixture changed to brilliant yellow. GO was achieved by centrifuging (10,000 rpm), washing with 15 mL of 10 wt.% HCl and deionized water, and freeze-drying. Finally, GO was redispersed in deionized water to form aqueous dispersion (2 mg mL^{-1}).

2.3. Preparation of C-MoS_2/N-G aerogel

In a typical synthesis, 0.2 g C-MoS_2 nanosheets were added into 60 mL GO dispersion, followed by ultrasonicating for 1 h. Subsequently, certain amount of $NH_3 \cdot H_2O$ solution was gradually dropped into the above mixture to control pH value (pH = 10.1) under constant stirring. The resulting solution was transferred into a 100 mL stainless steel autoclave for hydrothermal reaction at 180 °C for 24 h. After cooling naturally, the black cylinder of C-MoS_2/N-G hydrogel was taken out and washed with water for three times. The final product C-MoS_2/N-G aerogel was obtained by freeze-drying and annealing at 600 °C in Ar for 2 h.

2.4. Characterization

X-ray diffraction measurements were performed using an X'Pert PRO instrument with Cu $K\alpha$ radiation. Raman spectra were conducted on the Renishaw inVia Raman microscope under the excitation length of 532 nm. The morphologies and microstructures of